DOI: 10.4274/terh.galenos.2023.60024
J Tepecik Educ Res Hosp 2023;33(1):100-19

CLINICAL RESEARCH / KLİNİK ARAŞTIRMA

OPEN ACCESS

Comparative Transcriptome Analysis Identifies Target Genes for Treatment of IDH Wild-type Lower-grade Gliomas

Karşılaştırmalı Transkriptom Analizi ile Tanımlanan IDH Yabanıl-tip Düşük-gradeli Gliomların Tedavisine Yönelik Hedef Genler

Fadime Öztoprak[1], Zerrin Işık[2], Yavuz Oktay[3,4]

[1]Dokuz Eylül University, İzmir International Biomedicine and Genome Institute, İzmir, Turkey
[2]Dokuz Eylül University Faculty of Engineering, Computer Engineering Department, İzmir, Turkey
[3]İzmir Biomedicine and Genome Center, İzmir, Turkey
[4]Dokuz Eylül University Faculty of Medicine, Department of Medical Biology, İzmir, Turkey

Cite as: Öztoprak F, Işık Z, Oktay Y. Comparative Transcriptome Analysis Identifies Target Genes for Treatment of IDH Wild-type Lower-grade Gliomas. J Tepecik Educ Res Hosp 2023;33(1):100-19

Abstract

Objective: *Isocitrate dehydrogenase 1/2 (IDH 1/2)* mutations define a group of low-grade gliomas (LGGs) that display more favorable prognosis compared with LGGs without them. Although IDH wild-type (IDHwt) LGGs are classified as low-grade, they almost invariably progress to higher grades and rarely respond to aggressive treatment regimes. Here, we employed a comparative transcriptomic approach to identify key genes that could significantly contribute to the aggressive progression of IDHwt LGGs.

Methods: Using The Cancer Genome Atlas LGG cohort data and weighted gene coexpression network analysis methodology, we identified modules that correlated significantly with clinical features. We focused on modules that correlated with *telomerase reverse transcriptase (TERT)* promoter mutation status, as *TERT* promoter mutations are shared between glioblastomas and oligodendrogliomas, however, with two opposite prognostic outcomes. We selected module pathways shared between IDH mutant (IDHmt) and IDHwt LGGs and identified genes that were differentially expressed between the two groups.

Results: Several synaptic proteins are down-regulated in IDHwt compared with IDHmt, while *GNG12* and *VIPR2* are up-regulated. Finally, we identified known drugs that could target many of those genes and therefore could be tested against IDHwt LGGs.

Conclusion: Targeting of multiple candidate genes identified in this study could provide novel approaches toward the treatment of IDHwt LGGs.

Keywords: Low-grade gliomas, IDH 1, differential gene expression analysis, weighted gene co-expression network analysis, therapeutic target

Öz

Amaç: *İzositrat dehidrogenaz 1/2 (IDH 1/2)* mutasyonları, düşük-gradeli gliomların (LGG) daha iyi prognoza sahip bir alt grubunu tanımlar. IDH yabanıl-tip (IDHwt) LGG'ler düşük dereceli olarak sınıflandırılmalarına rağmen, neredeyse her zaman daha yüksek derecelere doğru ilerler ve agresif tedavi rejimlerine nadiren yanıt verirler. Burada, IDHwt LGG'lerin agresif ilerlemesine önemli ölçüde katkıda bulunan anahtar genleri belirlemek için karşılaştırmalı bir transkriptomik yaklaşım kullandık.

Address for Correspondence/Yazışma Adresi: Yavuz Oktay MD, İzmir Biomedicine and Genome Center, İzmir, Turkey. Dokuz Eylül University Faculty of Medicine, Department of Medical Biology, İzmir, Turkey
Phone: +90 232 299 41 00 **E-mail:** yavuz.oktay@deu.edu.tr
ORCID ID: orcid.org/0000-0002-0158-2693

Received/Geliş tarihi: 08.12.2022
Accepted/Kabul tarihi: 22.01.2023

©Telif Hakkı 2023 Sağlık Bilimleri Üniversitesi, İzmir Tepecik Eğitim ve Araştırma Hastanesi / İzmir Tepecik Eğitim ve Araştırma Hastanesi Dergisi, Galenos Yayınevi tarafından yayınlanmıştır.
©Copyright 2023 by the University of Health Sciences Turkey, İzmir Tepecik Training and Research Hospital / The Journal of Tepecik Education and Research Hospital published by Galenos Publishing House. Licensed by Attribution-NonCommercial 4.0 International (CC BY-NC 4.0).

Öz

Yöntem: Kanser Genom Atlası LGG kohort verilerini ve ağırlıklı gen ortak ifade ağı analizi metodolojisini kullanarak, klinik özelliklerle önemli ölçüde ilişkili olan modüller belirledik. *Telomeraz ters transkriptaz (TERT)* promotör mutasyon durumu ile ilişkili modüllere odaklandık, çünkü *TERT* promotör mutasyonları glioblastomlar ve oligodendrogliomlar arasında paylaşılsa da, bu iki gliom alttipi zıt prognostik özelliklere sahiptir. IDH mutantı (IDHmt) ve IDHwt LGG'ler arasında paylaşılan modül yolaklarını seçtik ve iki grup arasında diferansiyel olarak eksprese edilen genleri belirledik.

Bulgular: Çok sayıda sinaptik protein, IDHwt'de IDHmt'ye kıyasla aşağı regüle edilirken, *GNG12* ve *VIPR2* yukarı regüle edilmektedir. Son aşamada ise, bu genlerin birçoğunu hedef alabilecek ve dolayısıyla IDHwt LGG'lere karşı test edilebilecek bilinen ilaçları belirledik.

Sonuç: Bu çalışmada tanımlanan çoklu aday genlerin hedeflenmesi, IDHwt LGG'lerin tedavisine yönelik yeni yaklaşımlar sağlayabilir.

Anahtar Kelimeler: Düşük-dereceli gliomlar, IDH 1, diferansiyel gen ekspresyon analizi, ağırlıklı gen ortak ekspresyon ağ analizi, terapötik hedef

Introduction

Gliomas represent almost 80% of the primary brain tumors in adults. It constitutes a very heterogeneous group of neoplasms that differs in the context of age at diagnosis, location of the tumor, histological subtype, tumor invasiveness and malignancy, aptness to progression, and response to therapies. Gliomas have traditionally been divided into four grades and two groups: Grade I-II as low-grade gliomas, and grade III-IV as high-grade gliomas[1]. Grade IV gliomas glioblastomas (GBM) in particular, are the most common and aggressive form of glioma.

The advances in molecular biology and next-generation sequencing (NGS) lead to the identification of key molecular alteration gliomas. Co-deletion of chromosome arms 1p and 19q (1p/19q codeletion) was the first alteration that was identified in the 1990s[2]. It leads to oligodendroglial gliomas, is a prognostic factor, and a strong determinant of sensitivity to chemotherapy[3-5]. Mutations in isocitrate dehydrogenase (*IDH)1/IDH2* genes are diagnostic and prognostic markers that were identified for the first time in GBM[6,7], and later observed in myeloid malignancies[8], cholangiocarcinoma[9], and melanoma[10] among others[11,12]. They are observed in >70% of grade II-III gliomas [from now on referred to as lower-grade gliomas (LGGs)] and associated with alterations in epigenetic marks genome-wide and with altered cellular metabolism. The third one was two activating mutations in the *telomerase reverse transcriptase (TERT)* promoter (pTERT) [13]. pTERT mutations are observed in primary GBM, as well as in oligodendrogliomas, and they play an important role in tumorigenesis by helping tumor cells evade replicative crisis[14]. Until 2016, central nervous system (CNS) tumors were traditionally classified based mostly on the histological features. With better characterization of the molecular alterations thanks to advances in NGS, a new classification system was adopted, which takes into account both histological and molecular features such as IDH mutation status and 1p/19q codeletion status[15]. These alterations are not only important by using a tumor classification but are also important markers of patient survival and response to therapy. Eckel-Passow et al.[16] showed that in LGGs , the patients with only a TERT promoter mutation (considering 1p/19q-codeletion, IDH mutation, pTERT mutation) showed the poorest survival. Patients with IDH and pTERT mutations, indicating oligodendroglial histology, have the best survival. The Cancer Genome Atlas (TCGA) Research Network[17] has created a comprehensive catalog of cancer data at multi-omics level. TCGA has helped researchers study different tumor types at a deeper level, supporting the discovery of new biomarkers and helping further understanding of the mechanisms related to tumor formation, metastasis, subclassification of cancer types, therapy resistance or sensitivity, thus contributing to the diagnosis and treatment of cancer. Verhaak et al.[18] described a gene-expression-based system toward the molecular classification of GBMs and integrated multi-dimensional genomic data to establish patterns of somatic mutations and DNA copy number. Yang et al.[19] used a weighted gene coexpression network analysis (WGCNA) approach on glioblastoma data to explain the underlying molecular mechanisms and identify candidate biomarkers. The researchers proposed *CPNE6*, *HAPLN2*, *CMTM3*, *NMI*, *CAPG*, and *PSMB8* as liquid biopsy markers, and *NUSAP1* and *GPR65* as potential prognostic targets for gene therapy. Xu[20] identified differentially expressed genes (DEGs) between LGG and glioblastoma and proposed potential biomarkers and therapeutic targets for gliomas. Despite intense efforts over the past few decades, only minor improvements for treating diffuse gliomas have been made, and no complete cure of patients is still possible. However, it became clear that IDH mutant (IDHmt) gliomas, particularly those with 1p19q codeletion, have much better survival rates and responses to therapy. On the contrast, GBM are highly resistant to therapeutic approaches. The extensive heterogeneous (intra- and inter-tumoral) nature of GBM and

their highly invasive and infiltrative characteristics are the main challenges standing in the way of progress in treating GBM. While IDH wild-type (IDHwt) LGGs are not high grade, their survival is dismal, more similar to GBM than they are to IDHmt LGGs. Here, we performed a comparative analysis of transcriptomic data from LGG IDHmt and LGG IDHwt cohorts of TCGA to identify similarities and differences from a co-expression perspective. We detected gene modules that are likely to express simultaneously under different IDH mutation statuss. We observed correlations between these modules and the selected clinical features. Next, we determined which biological features are involved in clinically important modules by performing enrichment analysis of module genes using the Kyoto Encyclopedia of Genes and Genomes (KEGG) database. Comparison of pathway -enriched genes with differentially expressed ones led to a list of candidate genes that were mapped to pathways shared between IDHmt and IDHwt, albeit differently between the two groups. Finally, we screened gene-drug interaction databases to identify drugs and/or small molecules that could alter the expression levels of these candidate genes and hence could be particularly effective against IDHwt LGGs.

Materials and Methods

Data Collection and Preprocessing

Collection and preprocessing of transcriptomic data is performed using the TCGA Biolinks[21] package, which is created for integrative analysis with the GDC data. The relevant samples were searched and downloaded by "GDCquery" and "GDCdownload" functions respectively. The samples were prepared by "GDCprepare" function, and relevant clinical data were extracted from the Large Ranged Summarized Experiement Object. Gene expression data (RNA-sequencing) of lower-grade glioma patients were divided into sub-groups according to IDH mutation status (mt: mutated; wt: wild type) (Figure 1). The outlier samples were detected using the average method and manually excluded (Supplementary Figure 1). Finally, we have created two different expression matrices and two different data frames of clinical and molecular characteristics of patients. RNA-sequencing read counts do not show a normal distribution, so count data can be modeled with a poisson or negative binomial distribution[22]. Here, we followed the negative binomial distribution and normalized RNA-sequence data with the voom methodology[23]. The genes were filtered with the quantile method by setting the threshold value to 0.25. Before starting the analysis, the gene quality was checked.

Construction of the Weighted Gene Co-expression Network

We have constructed scale-free undirected co-expression networks using the WGCNA package in R[24]. We have used the "pickSoftThreshold" function to determine the soft threshold power beta based on the scale-free topology criterion. For WGCNA, the suggested β value is lowest showing R2 >0.80[25]. According to the suggested selection criteria, we have picked beta values as "6" for the TCGA IDHmt cohort and "12" for the TCGA IDHwt cohort (Supplementary Figure 2). Gene modules were constructed with a correlation network methodology (module size: 30, merge cut height: 0.25).

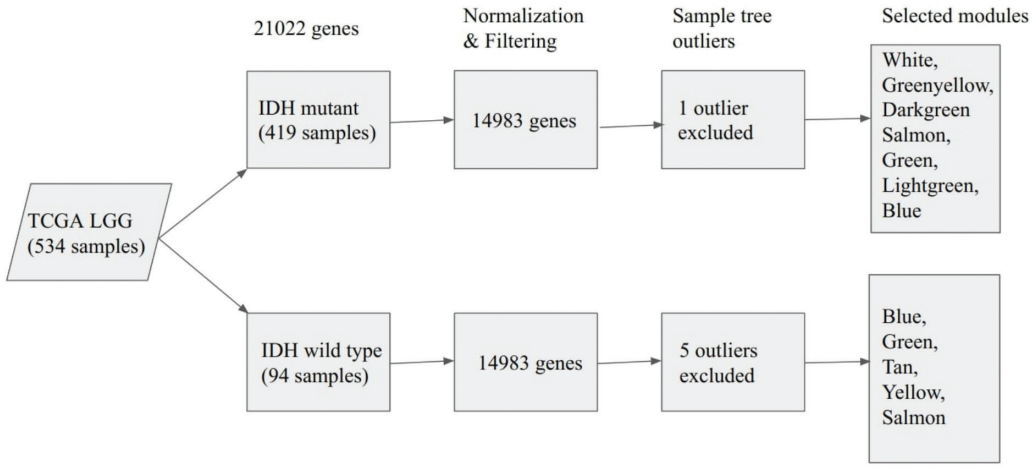


Figure 1. Module construction and clinically significant module detection by WGCNA.

WGCNA: Weighted gene co-expression network analysis, TCGA: The Cancer Genome Atlas, LGG: Lower-grade glioma, IDH: Isocitrate dehydrogenase

Identification of Clinically Significant Modules

After the module construction the relationship between module genes and external clinical traits has been observed using eigengene network methodology. Eigengene is the summary profile of the module. Basically, eigengenes were correlated with external traits (features) for the most significant associations. Originally, there were 110 features in the TCGA clinical data frame, but we have created a sub-data frame of 8 features according to the aim of this study. The features selected for this study are: Chr7gain. Chr10Loss, Chr19_20.co.gain, TERT.promoter.status, TERTexpression. log2, TERTexpression.status, ATRX.status, Telomere. Maintenance, BRAF.V600E.status. For further analysis, we have detected the modules that show strong positive and strong negative correlation with the TERT.promoter.status.

Statistical Analysis

We have listed the genes from modules of interest and converted gene names and synonyms to Entrez identifiers. We used the Database for Annotation, Visualization, and Integrated Discovery platform to perform enrichment analysis[26]. Functional annotation charts were downloaded. A summary of the KEGG pathways was curated in table format for comparison. Due to being enriched in similar pathways and correlated with the pTERT status inversely, we have further analyzed IDHwt blue and IDHmt greenyellow modules by mapping them on KEGG pathway schemes with a KEGG mapper[27]. We colored the KEGG objects according to their involvement status. The components enriched only in the IDHwt blue module were colored blue; the components enriched only in the IDHmt greenyellow module were colored green; the components enriched in both modules were colored red and the rest of the objects were kept in their default color.

Differential Gene Expression Analysis

We have performed differential gene expression analysis between normal tissue and LGG IDHmt samples; normal tissue and LGG IDHwt samples; LGG IDHmt and LGG IDHwt samples. Normal samples (solid tissue normal) were selected from the TCGA GBM cohort since the TCGA LGG cohort doesnot include normal samples. We used the "TCGAanalyze_DEA" function in the TCGABiolinks package using the "exactTest" method. The FDR threshold was set to 0.01 and the absolute logarithmic fold change (logFC) was set to 1 to identify DEGs. We have screened DEGs for the blue module on the normal tissue vs LGG IDHw, and the greenyellow module on the normal tissue vs LGG IDHmt. Additionally, we have listed the genes that were enriched in common pathways between greenyellow and blue modules. We focused on genes enriched only in the blue module for the next step as they were observed in different components of the same pathways.

Drug-gene Interactions

Using the Drug Gene Budger (DGB) tool[28], we have screened drugs that were changing the expression of selected genes accordingly. We have selected drugs that have inhibitory or activatory effects on up-regulated or down- regulated genes, respectively, using the CRowd Extracted Expression of Differential Signatures dataset[29].

Results

Pre-processing of TCGA LGG RNASeq Dataset and Construction of Weighted Gene Co-expression Networks

TCGA LGG RNASeq data subgroups based on their IDH mutation status were preprocessed separately. The TCGA LGG IDHmt subgroup consisted of 419 patients, and the TCGA LGG IDHwt subgroup consisted of 94 patients. Both the expression matrices contained 21,022 genes. After filtering and normalization steps, 14,893 genes were left. We have performed a sample-wise hierarchical clustering and detected one outlier sample and five outlier samples in the LGG IDHwt and LGG IDHmt subgroups, respectively. These outliers were excluded from the expression matrices. According to the clinical information, there were 92 pTERT-mutated samples and 143 pTERT wt samples in the IDHmt subgroup; 36 pTERT-mutated samples and 16 pTERT wt samples in the IDHwt subgroup that were recorded. pTERT mutation status was not available for the rest of the samples. We have constructed weighted gene expression networks using selected soft-thresholding powers (IDHmt subgroup: 6; IDHwt subgroup: 12). The modules were generated in the hierarchical clustering tree (dendrogram), and each module was labeled by different colors (Supplementary Figure 3). There were 28 modules constructed in the LGG IDHmt cohort, and 14 modules were constructed in the LGG IDHwt cohort. Genes that havenot been clustered in any module were collected in "Grey" modules in both cohorts (LGG IDHmt: 1055 genes, LGG IDHwt: 6314 genes).

Identification of Clinically Significant Modules

After the module construction, we performed a significance analysis to discover gene modules associated with the

clinical traits by observing module-trait relationship plots (Figure 2). We set correlation threshold values above 0.5 and below -0.5 to detect meaningful associations. We didnot observe any correlations with Chr19_20.co.gain or BRAF.V600E.status features for the LGG IDHmt subgroup. Hence, these columns are not shown in Figure 2, for simplicity. For the LGG IDHwt subgroup, blue module (# of genes: 1622, cor: 0.61, p-val: 2e-10), green module (# of genes: 655, cor: 0.60, p-val: 5e-10), and tan module (# of genes: 102, cor: 0.59, p-val: 9e-10) showed a positive correlation with TERT promoter mutation status. Yellow module (# of genes: 830, cor: -0.53, p-val: 7e-08) and salmon module (# of genes: 100, cor: -0.51, p-val: 4e-07) had negative correlation values that were below the threshold (Figure 2A). For the LGG IDHmt subgroup, green module (# of genes: 1032, cor: 0.86, p-val: 8e-124), salmon module (# of genes: 391, cor: 0.68, p-val: 2e-58), blue module (# of genes: 1354, cor: 0.54, p-val: 3e-33), darkgreen module (# of genes: 64, cor: 0.52, pval: 8e-31), and lightgreen module (# of genes: 106, cor: 0.52, p-val: 2e-30) showed positive correlation with TERT promoter mutation status. White module (# of genes: 36, cor: -0.64, p-val: 4e-50) and greenyellow module (# of genes: 538, cor: -0.57, p-val: 1e-37) showed negative correlation values that were below the threshold (Figure 2B).

Enrichment Analysis for Modules of Interest

Table 1 gives a summary of the KEGG pathway enrichment results. These results indicate that, in the IDHwt cohort, modules that are negatively correlated with the pTERT status (pTERT-) are enriched in immune -related pathways and those positively correlated (pTERT+) with the pTERT status are enriched in synaptic and glutamatergic pathways. In the IDHmt cohort, modules that are negatively correlated with the pTERT (pTERT-) status are enriched in cellular differentiation and proliferation, and synaptic pathways. Modules that are positively correlated with the pTERT status (pTERT+) are enriched in metabolomic and immune-related pathways. Interestingly blue module from the IDHwt cohort and greenyellow module from the IDHmt cohort are enriched in similar pathways, but their correlations with pTERT status are in opposite directions. We have investigated common pathways in KEGG to better understand the similarities and differences. We have identified 13 common pathways between the IDHmt greenyellow module and the IDHwt blue module related to synaptic pathways (Table 2). In the "Glutamatergic

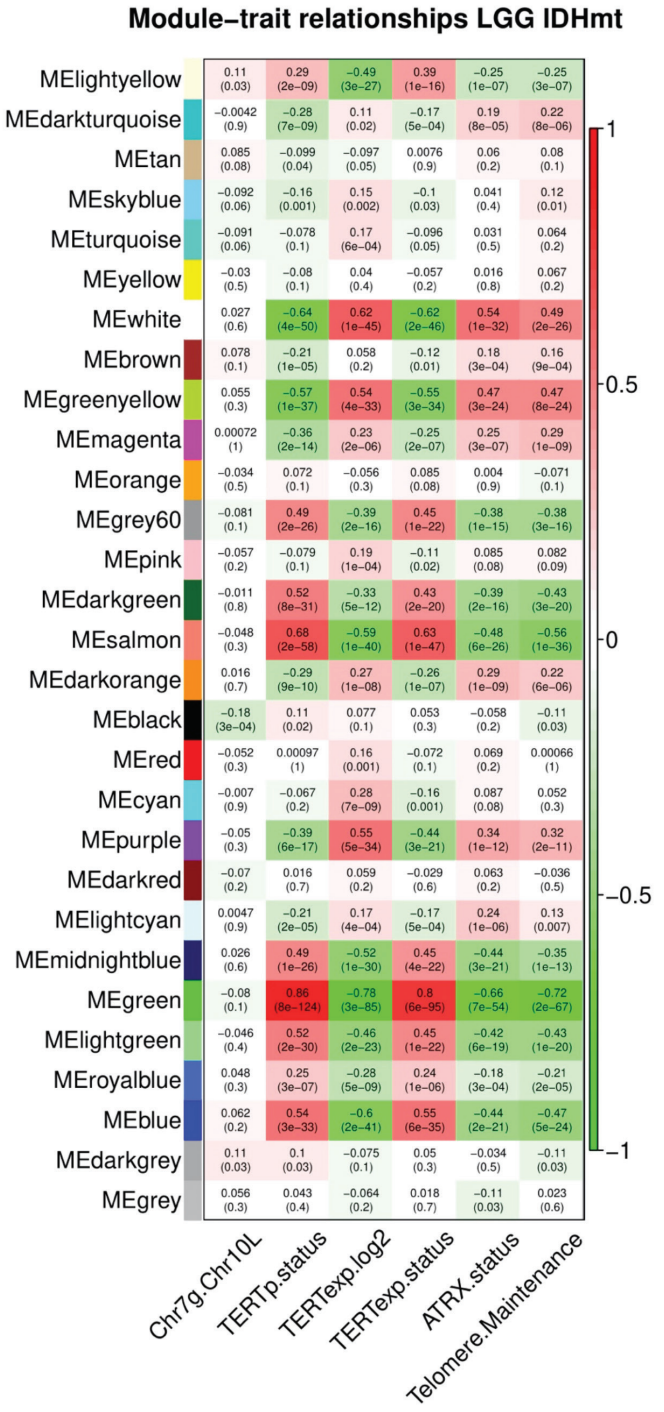


Figure 2A. Module-Trait relationships plot for LGG IDHmt samples

LGG: Lower-grade glioma, IDHmt: Isocitrate dehydrogenase mutated, Chr: Chromosome, g: Gain, L: loss, exp: Expression, TERTp: Telomerase Reverse Transcriptase promoter, ATRX: Alpha-thalassemia/mental retardation, X-linked, BRAF.V600E: mutation of the *BRAF* gene in which valine (V) is substituted by glutamic acid (E) at amino acid 600, upper numbers show Pearson correlation, and lower numbers show p-values

Synapse" pathway, glutamate ionotropic receptor NMDA type subunits were annotated in both modules, but in the IDHwt blue module, glutamate ionotropic receptor AMPA type subunit 1 (*GRIA1*) was also annotated. Glutamate metabotropic receptors were annotated in both the blue and greenyellow modules, but *GRM2* was annotated only in the IDHwt blue module. Other than *GRM2*, G protein alpha subunits (i1, i3 and o1) and adenylate cyclases (*ADCY1*, *ADCY5*) were also enriched in the IDHwt blue module. Cell migration and proliferation are promoted by glutamate receptors by allowing Ca^{2+} entrance into the cells (Supplementary Figure 4A).

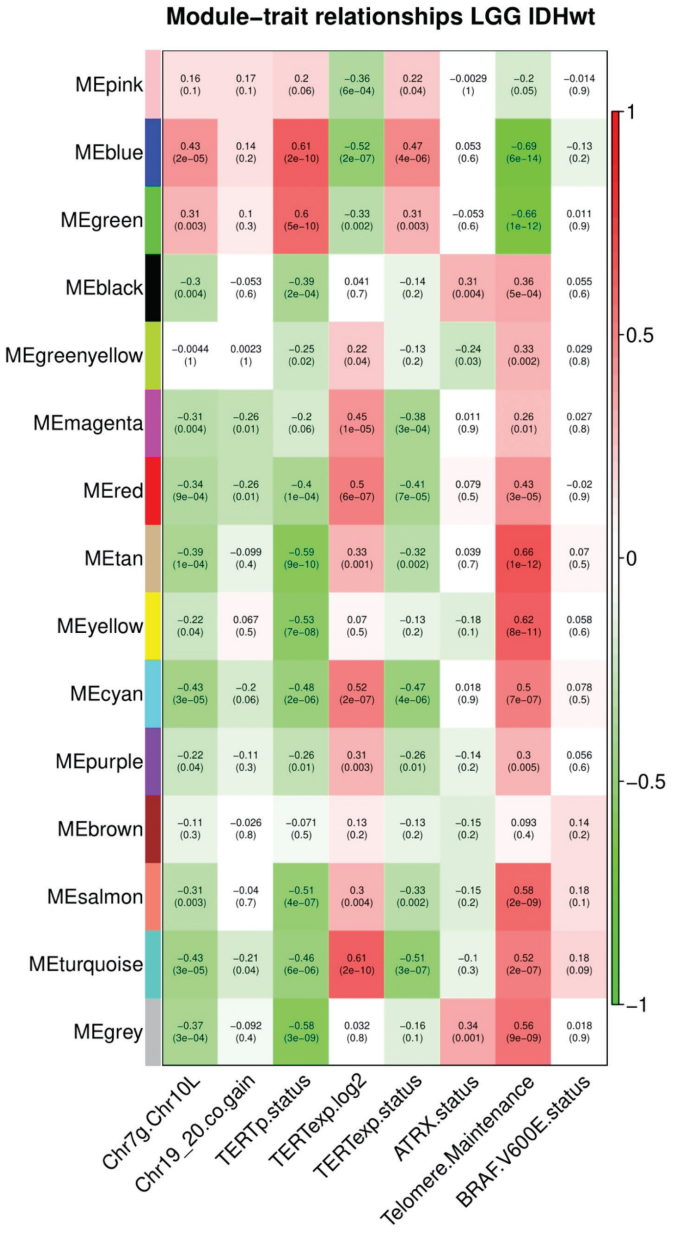


Figure 2B. Module-Trait relationships plot for LGG IDHwt samples

LGG: Lower-grade glioma, IDHwt: Isocitrate dehydrogenase wild-type, Chr: Chromosome, g: Gain, L: Loss, exp: Expression, TERTp: Telomerase Reverse Transcriptase promoter, ATRX: Alpha-thalassemia/mental retardation, X-linked, BRAF.V600E: mutation of the BRAF gene in which valine (V) is substituted by glutamic acid (E) at amino acid 600, upper numbers show Pearson correlation, and lower numbers show p-values

When adenylate cyclase is activated by G-protein-coupled receptors, it turns on PKA. This interaction also happens within the mitochondria in the "Retrograde endocannabinoid signaling" pathway (Supplementary Figure 4B). We observed potassium channel proteins in the retrograde endocannabinoid signaling pathway, GABAergic synapse, and cholinergic synapse pathways in the IDHwt blue module (Supplementary Figure 4C).

Differentially Expressed Genes

We have identified 3025 and 2804 genes that were differentially expressed in the LGG IDHmt subtype and in the LGG IDHwt subtype compared to normal samples, respectively. In addition we have identified 1958 genes that were differentially expressed in the LGG IDHwt subtype compared to the LGG IDHmt subtype. Screening the selected modules for the DEGs returned 206 and 984 genes for the IDHmt pTERT- greenyellow module and IDHwt pTERT+ blue module, respectively. We further identified 146 genes that were common between normal vs. IDHwt and IDHmt vs IDHwt DEGs. Fifty-three of these 146 DEGs were upregulated and 93 of them were downregulated.

The lowest logFC value was observed for the *GRIN3A* gene (IDHmt vs IDHwt -1.96; normal vs IDHwt -2.95) and the highest logFC value was observed for the *HPD* gene (IDHmt vs IDHwt 2.01; normal vs IDHwt 6.53). Interestingly, the logFC values for the IDHmt vs IDHwt and normal vs IDHwt groups were not very different for downregulated genes, but there were significant differences for upregulated genes. We have listed 182 genes in the IDHwt blue module and 54 genes in the IDHmt greenyellow module, which were enriched in common pathways; 143 and 27 of them were differentially expressed, respectively. 22 of 182 blue module genes were differentially expressed between IDHmt and IDHwt samples. 15 of 22 genes were also differentially expressed between normal vs IDHwt samples (Table 3).

Table 1. KEGG pathway enrichment of the selected modules

IDH mutation status	pTERT status (correlation)	Module	Term	p-value	Bonferroni
Wildtype	Negative	Yellow	hsa04060:Cytokine-cytokine receptor interaction	2.37E-10	7.29E-08
			hsa04064:NF-kappa B signaling pathway	8.00E-08	2.46E-05
			hsa04620:Toll-like receptor signaling pathway	1.68E-06	0.0005
			hsa04650:Natural killer cell mediated cytotoxicity	2.28E-06	0.0007
			hsa04062:Chemokine signaling pathway	2.62E-06	0.0008
		Salmon	hsa05235:PD-L1 expression and PD-1 checkpoint pathway in cancer	0.0106	0.8196
			hsa04660:T -cell receptor signaling pathway	0.0161	0.9265
			hsa04630:JAK-STAT signaling pathway	0.0501	0.9997
			hsa04662:B -cell receptor signaling pathway	0.0663	0.9999
			hsa04625:C-type lectin receptor signaling pathway	0.0997	0.9999
	Positive	Tan	hsa04621:NOD-like receptor signaling pathway	1.61E-10	1.34E-08
			hsa04622:RIG-I-like receptor signaling pathway	6.66E-06	0.0006
			hsa04625:C-type lectin receptor signaling pathway	0.0052	0.3486
			hsa04620:Toll-like receptor signaling pathway	0.0052	0.3486
			hsa04062:Chemokine signaling pathway	0.0399	0.9658
		Green	hsa04724:Glutamatergic synapse	1.07E-06	0.0003
			hsa04921:Oxytocin signaling pathway	3.44E-06	0.0009
			hsa04022:cGMP-PKG signaling pathway	4.03E-05	0.0116
			hsa04010:MAPK signaling pathway	4.49E-05	0.0129
			hsa04725:Cholinergic synapse	0.0004	0.1027
			hsa04728:Dopaminergic synapse	0.0005	0.1226
		Blue	hsa04721:Synaptic vesicle cycle	1.19E-18	3.77E-16
			hsa04727:GABAergic synapse	5.60E-13	1.77E-10
			hsa04724:Glutamatergic synapse	3.30E-11	1.04E-08
			hsa04723:Retrograde endocannabinoid signaling	5.64E-11	1.78E-08
			hsa04728:Dopaminergic synapse	5.40E-10	1.71E-07
			hsa04080:Neuroactive ligand-receptor interaction	8.20E-10	2.59E-07
			hsa04024:cAMP signaling pathway	9.60E-08	3.03E-05

Table 1. Continued

IDH mutation status	pTERT status (correlation)	Module	Term	p-value	Bonferroni
Mutant	Negative	White	hsa05202:Transcriptional misregulation in cancer	0.0537	0.9903
			hsa04024:cAMP signaling pathway	0.0682	0.9974
			hsa04014:Ras signaling pathway	0.0765	0.9988
		Greenyellow	hsa04724:Glutamatergic synapse	2.11E-08	4.87E-06
			hsa04080:Neuroactive ligand-receptor interaction	3.42E-06	0.0008
			hsa04721:Synaptic vesicle cycle	6.58E-06	0.0015
			hsa04727:GABAergic synapse	0.0001	0.0294
			hsa04723:Retrograde endocannabinoid signaling	0.0004	0.0825
			hsa04725:Cholinergic synapse	0.0032	0.5218
	Positive	Green	hsa00100:Steroid biosynthesis	0.0031	0.6146
			hsa01100:Metabolic pathways	0.0220	0.9990
			hsa00280:Valine, leucine and isoleucine degradation	0.0374	0.9999
			hsa00250:Alanine, aspartate, and glutamate metabolism	0.0416	0.9999
			hsa05231:Choline metabolism in cancer	0.0692	0.9999
		Salmon	hsa04146:Peroxisome	0.0001	0.0312
			hsa05022:Pathways of neurodegeneration - multiple diseases	0.0569	0.9999
			hsa04330:Notch signaling pathway	0.0954	1
			hsa04392:Hippo signaling pathway - multiple species	0.0998	1
		Blue	hsa04060:Cytokine-cytokine receptor interaction	1.81E-09	5.83E-07
			hsa04064:NF-kappa B signaling pathway	6.13E-09	1.98E-06
			hsa04662:B -cell receptor signaling pathway	6.13E-08	1.97E-05
			hsa04621:NOD-like receptor signaling pathway	3.70E-07	0.0001
			hsa04620:Toll-like receptor signaling pathway	4.39E-07	0.0001
		Darkgreen	hsa03010:Ribosome	5.58E-11	3.23E-09
		Lightgreen	hsa04015:Rap1 signaling pathway	0.0075	0.7415
			hsa01100:Metabolic pathways	0.0270	0.9927
			hsa04921:Oxytocin signaling pathway	0.0615	0.9999
			hsa04218:Cellular senescence	0.0634	0.9999
			hsa04390:Hippo signaling pathway	0.0644	0.9999

IDH: Isocitrate dehydrogenase, pTERT: Telomerase reverse transcriptase promoter, KEGG: Kyoto Encyclopedia of Genes and Genomes

Table 2. Common pathways between the IDH mutant (IDHmt) greenyellow module and IDH wild-type (IDHwt) blue module

IDHmt_greenyellow_pTERT-				IDHwt_blue_pTERT+			
Term	**Count**	**%**	**p-value**	**Term**	**Count**	**%**	**p-value**
hsa04724:Glutamatergic synapse	16	3.0246	0.0000	hsa04721:Synaptic vesicle cycle	36	2.2402	0
hsa04080:Neuroactive ligand-receptor interaction	24	4.5369	0.0000	hsa04727:GABAergic synapse	32	1.9913	0
hsa04721:Synaptic vesicle cycle	11	2.0794	0.0000	hsa04724:Glutamatergic synapse	34	2.1157	0
hsa04727:GABAergic synapse	10	1.8904	0.0001	hsa04723:Retrograde endocannabinoid signaling	39	2.4269	0
hsa04723:Retrograde endocannabinoid signaling	12	2.2684	0.0004	hsa04728:Dopaminergic synapse	35	2.1780	0.0000
hsa04725:Cholinergic synapse	9	1.7013	0.0032	hsa04080:Neuroactive ligand-receptor interaction	65	4.0448	0.0000
hsa04726:Serotonergic synapse	9	1.7013	0.0036	hsa04713:Circadian entrainment	29	1.8046	0.0000
hsa04360:Axon guidance	11	2.0793	0.0064	hsa04024:cAMP signaling pathway	43	2.6757	0.0000
hsa04024:cAMP signaling pathway	12	2.2684	0.0089	hsa04725:Cholinergic synapse	27	1.6801	0.0000
hsa04070:Phosphatidylinositol signaling system	6	1.1342	0.0606	hsa04070:Phosphatidylinositol signaling system	22	1.3690	0.0000
hsa04713:Circadian entrainment	6	1.1342	0.0606	hsa04726:Serotonergic synapse	24	1.4935	0.0000
hsa04728:Dopaminergic synapse	7	1.3233	0.0686	hsa04360:Axon guidance	30	1.8668	0.0002
hsa00330:Arginine and proline metabolism	4	0.7561	0.0952	hsa00330:Arginine and proline metabolism	9	0.5600	0.0441

pTERT- : Negatively correlated modules with TERT promoter status; pTERT+ : Positively correlated modules with TERT promoter status

Table 3. IDH wild-type blue module pathway-enriched DEGs

	logFC.Normal.vs. IDHwt.	**Normal**	**IDHwt**	**logFC.IDHmt.vs. IDHwt.**	**IDHmt**	**IDHwt**
SLC1A6	-2.2365	989.8	234.4494	-1.1974	514.5239	234.4494
GRIA2	-1.4941	15266	5926.5056	-1.0580	11873.9067	5926.5056
PLCB1	-1.4048	5828.6	2446.4719	-1.0379	4828.8660	2446.4719
GNG12	2.2310	1181.8	6309.8539	1.5414	2087.4952	6309.8539
GRIN3A	-2.9484	1916.6	272.1124	-1.9578	1032.8684	272.1124
SSTR1	-2.4319	2161.4	449.9550	-1.2700	1018.7297	449.9551
SSTR2	-2.5210	2055	399.4607	-1.7434	1284.4665	399.4607
CHRNA4	-1.6524	2051.6	749.1685	-1.0276	1409.4377	749.1685
GABRB3	-2.2102	9864.4	2436.4719	-1.0300	4725.7607	2436.4719
GABRA3	-2.1735	1813.8	444.5843	-1.5058	1251.0909	444.5843
PDYN	-2.1334	5622.8	1506.6517	1.1126	645.9139	1506.6517
VIPR2	2.3059	329.6	1830.6180	-1.5287	4821.8445	1830.6180
CHRM4	-2.3974	334.2	70.5056	-1.022	136.3301	70.5056
ATP6V1G2	-2.0278	13698.6	3727.4045	-1.0769	7554.8421	3727.4045
GNAL	-2.2018	2163.6	530.2809	-1.0779	1077.7105	530.2809

DEGs: Differentially expressed genes, IDHmt: Isocitrate dehydrogenase mutated, IDHwt: Isocitrate dehydrogenase wild-type, logFC: log-fold change. Genes that were enriched in the IDH wild-type blue module, but not in the IDH mutant greenyellow module are shown in bold.

Drug-gene Interactions

Among the 15 genes that were common between normal vs IDHmt and IDHmt vs IDHwt DEGs, 6 of them were enriched only in the blue module: *GRIA2*, *PLCB1*, *GNG12*, *GABRA3*, *PDYN*, and *GNAL*. We excluded PDYN as its expression pattern was not suitable for our hypothesis. *GNG12* was upregulated at IDHwt samples compared with IDHmt and normal samples, whereas the others were downregulated. We have listed inhibitory drugs / small molecules for *GNG12* and activatory drugs / small molecules for *GRIA2*, *PLCB1*, *GNG12*, *GABRA3*, and *GNAL*. Since *GNG12* was the most interesting candidate target, we have compared listed drugs for *GNG12* with drugs targeting other candidates (Table 4). As cisplatin, imatinib, vanadium pentoxide, and vemurafenib affect the expression of four out of five listed genes (including *GNG12*), these compounds were identified as potential therapeutics.

Discussion

Despite the efforts toward better understanding and treating gliomas in the last decades, many questions need to be answered and a great need for new treatments. In this study, we aimed to understand co-expressional dissimilarities, as well as shared pathways, between LGG IDHmt and LGG IDHwt subgroups. Although both subgroups are classified under the low-grade glioma category, their progression and survival times are extremely different. Among LGGs, the most favorable survival rate is observed when *IDH1/2* and pTERT mutations are present together with 1p19q codeletion (IDHmt / pTERTwt / 1p19q-codeleted), and the worst survival rate is observed when only pTERT mutation is present (IDHwt / pTERTmutant / 1p19q-intact)[16,30]. Here, we focused on the transcriptomic basis of these discrepancies with a co-expressional perspective to explore related biological

Table 4. Drug-gene interaction table for IDH wild -type blue module pathway-enriched DEGs

Drug Name	*GNG12*	*GRIA2*	*PLCB1*	*GABRA3*	*GNAL*
1,25 dihydroxyvitamin d	x				
4-hydroxynonenal	x		x		x
Adenosine triphosphate	x	x		x	
Alfacalcidol	x				
Aminolevulinic acid	x				x
Androstanolone	x				
Aplidin	x				x
Apratoxin a	x				
Bexarotene	x	x			
Bisphenol a	x		x	x	
Cediranib	x			x	
Cetuximab	x				
Chlorpyrifos	x		x		
Cisplatin	x		x	x	x
Clinafloxacin	x				
Cytarabine	x				
Diclofenac	x	x			x
Doxorubicin	x	x			x
Doxycycline	x				
Estradiol	x		x		
Harman	x				
Imatinib	x		x	x	x
Interferon beta-1a	x				
Interferon gamma-1b	x				x
Mesalazine	x		x		
Metformin	x				x

Table 4. Continued

Drug Name	*GNG12*	*GRIA2*	*PLCB1*	*GABRA3*	*GNAL*
Nickel	x				
Plx4032	x		x	x	
Puromycin, ec50, 1 d	x			x	
Puromycin, ec50, 5 d	x				
Resveratrol	x				
Sapphyrin pci-2050	x				
Tibolone	x				
Triiodothyronine-(13c6) hydrochloride (t3 thyronine)	x	x			
Trovafloxacin	x				
Vanadium pentoxide	x	x		x	x
Vemurafenib	x	x	x	x	
Vx	x				
Y15	x				

DEGs: Differentially expressed genes, Drugs that affect the expression of ⅘ genes, including GNG12, are shown in bold.

pathways and their components, and to extract information about mechanisms correlated with selected clinical features. Previously, CNS tumors were classified based on histology. The advancements in the NGS technologies allowed the researchers to profile tumor tissues at the molecular level, revealing the importance of such aberrations. In gliomas specifically, *IDH* mutation status was found to be a deterministic aberration (biomarker) and likely the earliest oncogenic change during gliomagenesis. While IDHmt gliomas respond well to therapies, IDHwt gliomas have dismal prognosis and eventually progress to GBM[31-33]. Understanding the differences between the two groups will not only provide more insights into the disease mechanisms, but also help designing novel and more effective therapies to prevent cancer progression. We applied a weighted gene co-expression analysis approach and identified modules correlated with clinical features of interest. The "Chr7gain. Chr10Loss" and "BRAF.V600E.status" clinical features showed correlations only with the IDHwt subtype (Figure 2A, B). Chr7p gain and loss of Chr10q are hallmarks of GBM and likely indicate a subgroup within IDHwt LGGs that are destined to progress to the classical type of glioblastoma. Ozawa et al.[34] computationally identified *PDGFA* (chr7) and *PTEN* (chr10) as driving initial nondisjunction events in non-GCIMP GBM. PDGFA mediates signaling pathways in the regulation of growth and survival of the cells, and *PTEN* codes for an enzyme that plays a role in tumor suppression. *BRAF* gene produces B-raf protein, which is involved in direct cell growth[35]. V600E stands for the amino acid substitution at position 600 [from valine (V) to glutamic acid (E)][36]. BRAF.V600E status is identified as a key driver in certain brain tumors and tumor metastasis (pilocytic astrocytomas, pleomorphic xanthoastrocytoma, ganglioma, and glioblastoma)[37]. As pTERT mutations are present in both oligodendrogliomas and GBM, two tumor types with opposite prognoses, we decided to identify similarities and differences between IDHwt and IDHmt LGGs with respect to the pTERT mutation status and selected modules of interest accordingly. We applied enrichment analysis for modules whose correlation value was above 0.5 or below -0.5 (Table 1). IDHwt yellow and salmon modules, which are negatively correlated with pTERT status, were enriched in immune -related pathways. On the other hand, the IDHmt blue module, which is enriched in immune -related pathways, showed a positive correlation with pTERT status. The immune system is a major component of the tumor microenvironment and is central to tumor progression and invasion. This observation reflects differences in the immune response to IDHwt and IDHmt tumors and could be explained by differences in tumor antigens, effects of 2-hydroxyglutarate on immune cells, or modulation of tumor-associated immune responses by different oncogenic processes in two tumor types, among others. IDHwt modules (green and blue) that were positively correlated with pTERT were enriched in synaptic pathways. On the other hand, in the IDHmt subgroup, the greenyellow module was enriched in synaptic pathways and negatively correlated with the pTERT status. We identified 13 common pathways between the IDHwt pTERT+ blue module and the

IDHmt pTERT- greenyellow module (Table 2). We observed that different sub-components of these pathways were enriched in the blue module compared to the greenyellow module. Glutamatergic synapse, circadian entrainment, and dopaminergic synapse pathways were particularly interesting, as α-amino-3-hydroxy-5-methylisoxazole-4-propionic acid (AMPA) glutamate receptor (AMPAR) and PKC/ERK signaling pathways are involved in the blue module, but not in the greenyellow module (Supplementary Figures 4A, E, F). AMPA receptors play a role in the glioma growth[38].

Our results showed that *GNG12* (up-regulated), *GNAL*, *GABRA3*, *GRIA2*, and *PLCB1* (down-regulated) genes were enriched in the IDHwt blue module, but not in the IDHmt greenyellow module. Most of the genes were down-regulated (except *GNG12*) in normal vs. LGG IDHmt and normal vs IDHwt comparisons.

GNG12 is a member of the G-protein family and it plays a role in cellular functions such as cell division, differentiation, and metastasis[39,40]. Liu et al.[41] showed that the proliferation and migration of glioma cells were correlated with *GNG12* expression. Our results indicate that *GNG12* expression is lowest in normal samples followed by IDHmt gliomas and it was the highest in IDHwt gliomas. *GNAL* encodes a stimulatory G protein alpha subunit. A study by Zhang et al. [42] related *GNAL* expression levels with gliomas. They identified 24 genes, including *GNAL*, that are related to glioma grade and prognosis. The expression of GNAL was inversely correlated with the glioma grade. Our results show that *GNAL* expression is the lowest in IDHwt gliomas followed by IDHmt gliomas and normal samples. Another interesting finding in the glutamatergic synapse pathway is the involvement of PKC/ERK pathway through phospholipase C beta 1 (*PLCB1*). *PLCB1* is correlated with glioma grade and plays a role in maintaining a normal or less aggressive glioma phenotype[43]. We observed that *PLCB1* was downregulated in the IDHwt subgroup. Patil et al.[44] showed that *GABRA3* expression was down-regulated in LGGs compared to normal samples and it was the lowest in GBMs. They evaluated TCGA and Cancer Cell Line Encyclopedia glioma data from a global RNA-editome perspective and found that exogenously produced and edited GABRA3 effectively prevented glioma cells from migration and invasion, but the unedited GABRA3 did not. High-grade gliomas release high concentrations of glutamate and enhance their malignant[45,46] and invasive behavior[47,48]. Our results showed that *GRIA2* (Glutamate Ionotropic Receptor AMPA Type Subunit 2) was enriched in the blue module but not in the greenyellow module. Differential gene expression analysis showed that this gene is down-regulated in IDHwt LGGs compared with IDHmt LGGs and normal samples (Table 3). In parallel with our results, van Vuurden et al.[49] showed that expression of AMPA receptor (*GRIA1-4*) was decreased by glioma grade (normal>LGG>GBM). The subunit encoded by *GRIA2* is contingent on RNA editing and it is thought to make the channel impermeable for Ca^{2+} (50). Ca^{2+} concentration is important in the intracellular space as it excites Ca^{2+}-dependent signal transduction pathways such as AKT[51], ERK/MAP kinase[52], and PKA[53], which are involved in cell proliferation and migration. Ramaswamy et al.[54] showed that AMPA-R enhances the invasion in GBM and ERK signaling affects the expression of calcium-permeable AMPA-R. Lu et al.[55] suggested *PLCB1* as a candidate biomarker for high -grade gliomas. They showed a correlation between *PLCB1* expression and the patient survival; an inverse correlation between *PLCB1* expression and the pathological grade of glioma. Our results indicated a decrease in the expression of the *PLCB1* in normal samples compared with the IDHmt subtype, and the lowest expression was in the IDHwt subtype. To summarize, the expression patterns of these candidate genes seem to promote a more GBM-like phenotype (aggressive behavior). Using the DGB tool, we listed small molecules/drugs that affect the expression levels of these candidate genes. We searched for inhibitory drugs for the expression of *GNG12* and activator drugs for *GNAL*, *GABRA3*, *GRIA2*, and *PLCB1* (Table 4). We noticed that cisplatin, imatinib, vanadium pentoxide and vemurafenib affect the expression of four out of the five listed genes. Wang et al.[56] showed active performance and acceptable toxicity of the combined treatment of cisplatin and temozolomide in recurrent GBMs. Enríquez Pérez et al.[57] showed that cisplatin treatment was beneficial in the treatment of GL261 glioma-bearing C57BL/6 mice, but not GL261-bearing NOD-scid IL2rγnull (NSG) mice. However, the combination of cisplatin with immunotherapy did not yield improved survival. Ferrari et al.[58] proposed a new platinum-based prodrug as an alternative for cisplatin and its analogs and showed its effectiveness in the U251 cell line. Holdhoff et al.[59] showed that imatinib increases the radiosensitivity in human GBM by disturbing the autocrine PDGF/PDGFR loop. We are not aware of any study of vanadium pentoxide treatment for glioma; however, Das et al.[60] reported proliferation inhibition of different cancer cell lines (B16F10, A549, and PANC1) which were treated with vanadium pentoxide nanoparticles (V2O5 NPs: 30-60 nm). Additionally, they showed a significant improvement in the survival of melanoma-bearing C57BL6/J

mice after treatment with V2O5 NPs compared to untreated tumor bearing mice. Vemurafenib is a selective inhibitor of BRAFV600; Kaley et al.[61] reported results of the VE-BASKET study, in which patients with BRAFV600-mutant gliomas received vemurafenib daily; they reported that the efficacy of vemurafenib varies qualitatively by histologic subtype. Nicolaides et al.[62] showed that vemurafenib has promising anti-tumor activity in recurrent or progressive BRAFV600E-positive pediatric gliomas with manageable toxicity (Phase I results, Phase II ongoing). Del Bufalo et al.[63] also suggested vemurafenib as a treatment option for pediatric low-grade gliomas carrying BRAFV600E. We also propose these drugs, alone or in combination, as possible treatments specifically for IDHwt LGGs.

Study Limitations

In this study, we used publicly available RNA-seq data from a well-characterized cohort. While the number of samples was quite high for the IDHmut LGG group, it was much lower for the IDHwt-pTERTwt subgroup, with 16 samples. Another limitation was related to the interrogation of possible drug candidates that could target many genes in our candidate gene list. As drug-gene interaction data were available for cell lines from cancers other than gliomas, we had to rely on such data. With the possible generation of similar data for glioma cell lines, we can be able to overcome this limitation and determine how it compared to our current findings.

Conclusion

In this study, we have determined potential therapeutic target candidates for IDHwt LGGs. Although these targets need to be validated experimentally, with the help of computational analyses, our study prioritizes potential targets for further investigation.

Acknowledgments

Fadime Öztoprak acknowledges TÜBİTAK 2211-C, YÖK 100/2000, and KYK scholarship programs. Computational analyses reported in this paper were partially performed at TUBITAK ULAKBIM, High Performance and Grid Computing Center (TRUBA resources). Yavuz Oktay is supported by the GEBIP young investigator award of the Turkish Academy of Sciences (TÜBA). This study was supported by TUBITAK grant 117Z981.

Ethics

Ethics Committee Approval: This study does not require ethics committee approval.

Informed Consent: N/A

Peer-review: Externally peer-reviewed.

Authorship Contributions

Concept: F.Ö., Z.I., Y.O., Design: F.Ö., Z.I., Y.O., Data Collection or Processing: F.Ö., Z.I., Analysis or Interpretation: F.Ö., Z.I., Y.O., Literature Search: F.Ö., Y.O., Writing: F.Ö., Z.I., Y.O.

Conflict of Interest: No conflict of interest was declared by the authors.

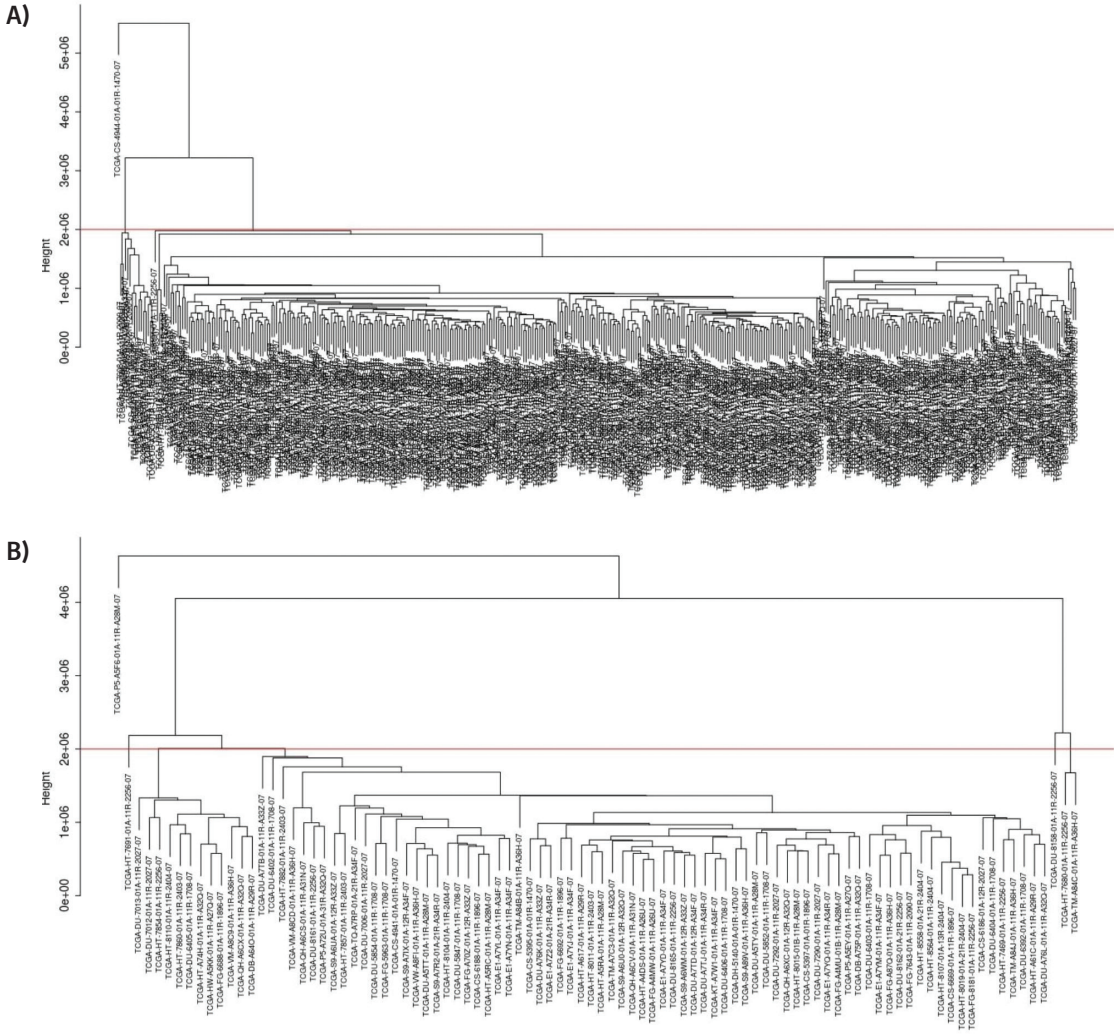
Financial Disclosure: This study was supported by TUBITAK grants 214S097 and 117Z981.

References

1. Louis DN, Ohgaki H, Wiestler OD, et al. The 2007 WHO classification of tumours of the central nervous system. Neuropathol 2007;114:97-109.
2. Reifenberger J, Reifenberger G, Liu L, James CD, Wechsler W, Collins VP. Molecular genetic analysis of oligodendroglial tumors shows preferential allelic deletions on 19q and 1p. Am J Pathol 1994;145:1175-90.
3. Jenkins RB, Blair H, Ballman KV, et al. A t(1;19)(q10;p10) mediates the combined deletions of 1p and 19q and predicts a better prognosis of patients with oligodendroglioma. Cancer Res 2006;66:9852-61.
4. Cairncross G, Wang M, Shaw E, et al. Phase III trial of chemoradiotherapy for anaplastic oligodendroglioma: long-term results of RTOG 9402. J Clin Oncol 2013;31:337-43.
5. van den Bent MJ, Brandes AA, Taphoorn MJ, et al. Adjuvant procarbazine, lomustine, and vincristine chemotherapy in newly diagnosed anaplastic oligodendroglioma: long-term follow-up of EORTC brain tumor group study 26951. J Clin Oncol 2013;31:344-50.
6. Parsons DW, Jones S, Zhang X, et al. An integrated genomic analysis of human glioblastoma multiforme. Science 2008;321:1807-12.
7. Yan H, Parsons DW, Jin G, et al. IDH1 and IDH2 mutations in gliomas. N Engl J Med 2009;360:765-73.
8. Marcucci G, Maharry K, Wu YZ, et al. IDH1 and IDH2 gene mutations identify novel molecular subsets within de novo cytogenetically normal acute myeloid leukemia: a Cancer and Leukemia Group B study. J Clin Oncol 2010;28:2348-55.
9. Amary MF, Bacsi K, Maggiani F, et al. IDH1 and IDH2 mutations are frequent events in central chondrosarcoma and central and periosteal chondromas but not in other mesenchymal tumours. J Pathol 2011;224:334-43.
10. Shibata T, Kokubu A, Miyamoto M, Sasajima Y, Yamazaki N. Mutant IDH1 confers an in vivo growth in a melanoma cell line with BRAF mutation. Am J Pathol 2011;178:1395-402.
11. Amary MF, Damato S, Halai D, et al. Ollier disease and Maffucci syndrome are caused by somatic mosaic mutations of IDH1 and IDH2. Nat Genet 2011;43:1262-5.
12. Pansuriya TC, van Eijk R, d'Adamo P, et al. Somatic mosaic IDH1 and IDH2 mutations are associated with enchondroma and spindle cell hemangioma in Ollier disease and Maffucci syndrome. Nat Genet 2011;43:1256-61.

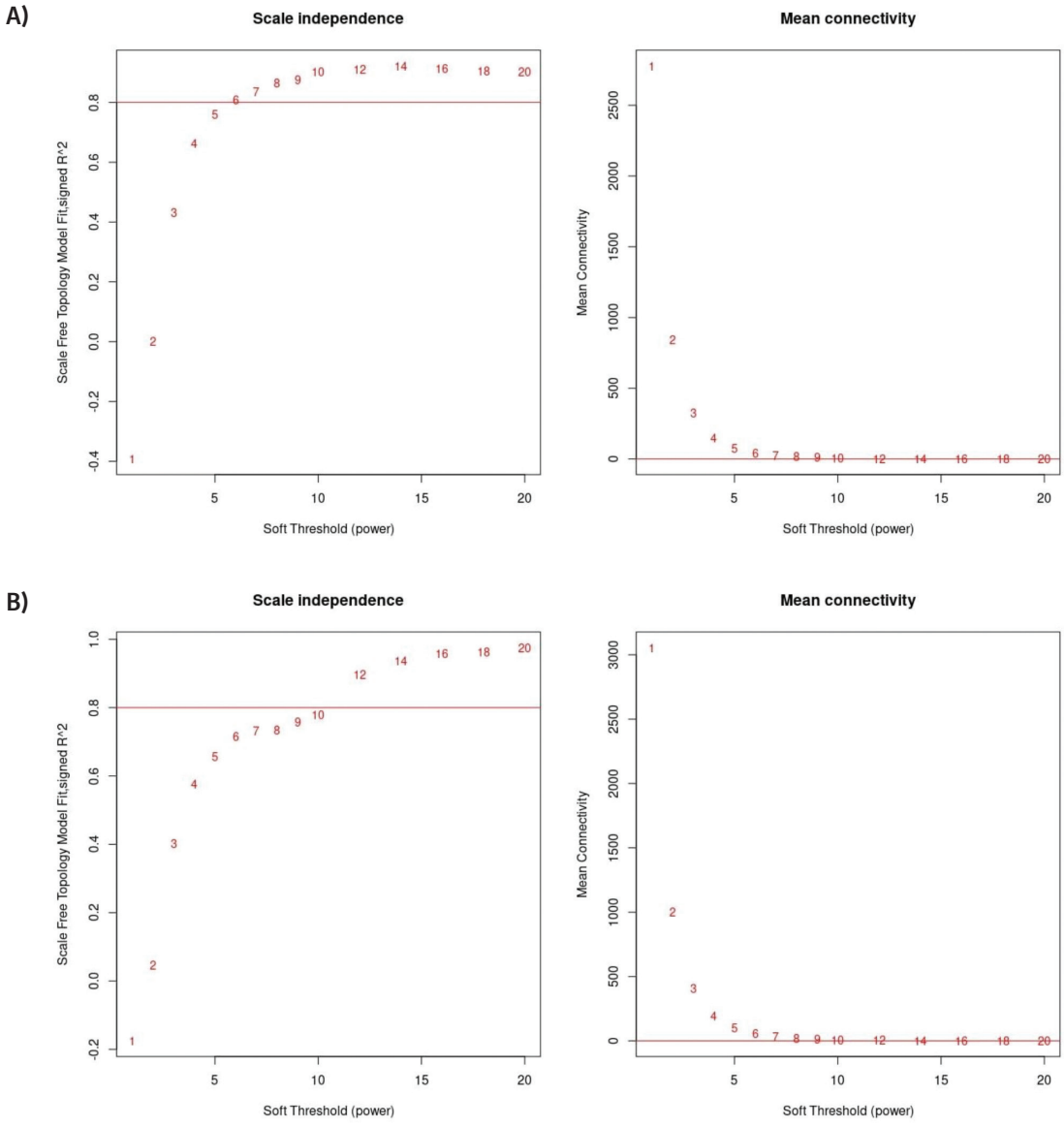
13. Vinagre J, Pinto V, Celestino R, et al. Telomerase promoter mutations in cancer: an emerging molecular biomarker? Virchows Arch 2014;465:119-33.
14. Killela PJ, Reitman ZJ, Jiao Y, et al. TERT promoter mutations occur frequently in gliomas and a subset of tumors derived from cells with low rates of self-renewal. Proc Natl Acad Sci 2013;110:6021-6.
15. Louis DN, Perry A, Reifenberger G, et al. The 2016 World Health Organization Classification of Tumors of the Central Nervous System: a summary. Acta Neuropathol 2016;131:803-20.
16. Eckel-Passow JE, Lachance DH, Molinaro AM, et al. Glioma Groups Based on 1p/19q, IDH, and TERT Promoter Mutations in Tumors. N Engl J Med 2015;372:2499-508.
17. Cancer Genome Atlas Research Network. Comprehensive genomic characterization defines human glioblastoma genes and core pathways. Nature 2008;455:1061-8.
18. Verhaak RG, Hoadley KA, Purdom E, et al. Integrated genomic analysis identifies clinically relevant subtypes of glioblastoma characterized by abnormalities in PDGFRA, IDH1, EGFR, and NF1. Cancer Cell 2010;17:98-110.
19. Yang Q, Wang R, Wei B, et al. Candidate Biomarkers and Molecular Mechanism Investigation for Glioblastoma Multiforme Utilizing WGCNA. Biomed Res Int 2018;2018:4246703.
20. Xu B. Prediction and analysis of hub genes between glioblastoma and low-grade glioma using bioinformatics analysis. Medicine (Baltimore) 2021;100:e23513.
21. Colaprico A, Silva TC, Olsen C, et al. TCGAbiolinks: an R/Bioconductor package for integrative analysis of TCGA data. Nucleic Acids Res 2016;44:e71.
22. de Torrenté L, Zimmerman S, Suzuki M, Christopeit M, Greally JM, Mar JC. The shape of gene expression distributions matter: how incorporating distribution shape improves the interpretation of cancer transcriptomic data. BMC Bioinformatics 2020;21:562.
23. Law CW, Chen Y, Shi W, Smyth GK. voom: Precision weights unlock linear model analysis tools for RNA-seq read counts. Genome Biol 2014;15:R29.
24. Langfelder P, Horvath S. WGCNA: an R package for weighted correlation network analysis. BMC Bioinformatics 2008;9:559.
25. Zhang B, Horvath S. A general framework for weighted gene co-expression network analysis. Stat Appl Genet Mol Biol 2005;4:Article17.
26. Sherman BT, Hao M, Qiu J, et al. DAVID: a web server for functional enrichment analysis and functional annotation of gene lists (2021 update). Nucleic Acids Res 2022;50:W216-21.
27. Kanehisa M, Sato Y, Kawashima M. KEGG mapping tools for uncovering hidden features in biological data. Protein Sci 2022;31:47-53.
28. Wang Z, He E, Sani K, Jagodnik KM, Silverstein MC, Ma'ayan A. Drug Gene Budger (DGB): an application for ranking drugs to modulate a specific gene based on transcriptomic signatures. Bioinformatics 2019;35:1247-8.
29. Wang Z, Monteiro CD, Jagodnik KM, et al. Extraction and analysis of signatures from the Gene Expression Omnibus by the crowd. Nat Commun 2016;7:12846.
30. Ostrom QT, Cioffi G, Gittleman H, et al. CBTRUS Statistical Report: Primary Brain and Other Central Nervous System Tumors Diagnosed in the United States in 2012-2016. Neuro Oncol 2019;21:v1-v100.
31. Gelman SJ, Naser F, Mahieu NG, et al. Consumption of NADPH for 2-HG Synthesis Increases Pentose Phosphate Pathway Flux and Sensitizes Cells to Oxidative Stress. Cell Rep 2018;22:512-22.
32. Nobusawa S, Watanabe T, Kleihues P, Ohgaki H. IDH1 mutations as molecular signature and predictive factor of secondary glioblastomas. Clin Cancer Res 2009;15:6002-7.
33. Ohgaki H, Dessen P, Jourde B, et al. Genetic pathways to glioblastoma: a population-based study. Cancer Res 2004;64:6892-9.
34. Ozawa T, Riester M, Cheng YK, et al. Most human non-GCIMP glioblastoma subtypes evolve from a common proneural-like precursor glioma. Cancer Cell 2014;26:288-300.
35. Sithanandam G, Kolch W, Duh FM, Rapp UR. Complete coding sequence of a human B-raf cDNA and detection of B-raf protein kinase with isozyme specific antibodies. Oncogene 1990;5:1775-80.
36. Davies H, Bignell GR, Cox C,. Mutations of the BRAF gene in human cancer. Nature 2002;417:949-54.
37. Kaley T, Touat M, Subbiah V, et al. BRAF Inhibition in *BRAF*^{V600}-Mutant Gliomas: Results From the VE-BASKET Study. J Clin Oncol 2018;36:3477-84.
38. Venkataramani V, Tanev DI, Strahle C, et al. Glutamatergic synaptic input to glioma cells drives brain tumour progression. Nature 2019;573:532-8.
39. Morishita R, Nakayama H, Isobe T, et al. Primary structure of a gamma subunit of G protein, gamma 12, and its phosphorylation by protein kinase C. J Biol Chem 1995;270:29469-75.
40. Asano T, Morishita R, Ueda H, Kato K. Selective association of G protein beta(4) with gamma(5) and gamma(12) subunits in bovine tissues. J Biol Chem 1999;274:21425-9.
41. Liu R, Liu Z, Zhao Y, et al. GNG12 as A Novel Molecular Marker for the Diagnosis and Treatment of Glioma. Front Oncol 2022;12:726556.
42. Zhang D, Zhao J, Han C, Liu X, Liu J, Yang H. Identification of hub genes related to prognosis in glioma. Biosci Rep 2020;40:BSR20193377.
43. Ratti S, Marvi MV, Mongiorgi S, et al. Impact of phospholipase C β1 in glioblastoma: a study on the main mechanisms of tumor aggressiveness. Cell Mol Life Sci 2022;79:195.
44. Patil V, Pal J, Mahalingam K, Somasundaram K. Global RNA editome landscape discovers reduced RNA editing in glioma: loss of editing of gamma-amino butyric acid receptor alpha subunit 3 (GABRA3) favors glioma migration and invasion. PeerJ 2020;8:e9755.
45. Rzeski W, Turski L, Ikonomidou C. Glutamate antagonists limit tumor growth. Proc Natl Acad Sci 2001;98:6372-7.
46. Yoshida Y, Tsuzuki K, Ishiuchi S, Ozawa S. Serum-dependence of AMPA receptor-mediated proliferation in glioma cells. Pathol Int 2006;56:262-71.
47. Takano T, Lin JH, Arcuino G, Gao Q, Yang J, Nedergaard M. Glutamate release promotes growth of malignant gliomas. Nat Med 2001;7:1010-5.
48. Ishiuchi S, Tsuzuki K, Yoshida Y, et al. Blockage of Ca(2+)-permeable AMPA receptors suppresses migration and induces apoptosis in human glioblastoma cells. Nat Med 2002;8:971-8.
49. van Vuurden DG, Yazdani M, Bosma I, et al. Attenuated AMPA receptor expression allows glioblastoma cell survival in glutamate-rich environment. PLoS One 2009;4:e5953.
50. Barbon A, Barlati S. Glutamate receptor RNA editing in health and disease. Biochemistry (Mosc) 2011;76:882-9.
51. Ishiuchi S, Yoshida Y, Sugawara K, et al. Ca2+-permeable AMPA receptors regulate growth of human glioblastoma via Akt activation. J Neurosci 2007;27:7987-8001.
52. Wiegert JS, Bading H. Activity-dependent calcium signaling and ERK-MAP kinases in neurons: a link to structural plasticity of the nucleus and gene transcription regulation. Cell Calcium 2011;49:296-305.
53. Danbolt NC. Glutamate uptake. Prog Neurobiol 2001;65:1-105.
54. Ramaswamy P, Dalavaikodihalli Nanjaiah N, Prasad C, Goswami K. Transcriptional modulation of calcium-permeable AMPA receptor subunits in glioblastoma by MEK-ERK1/2 inhibitors and their role in invasion. Cell Biol Int 2020;44:830-7.

55. Lu G, Chang JT, Liu Z, Chen Y, Li M, Zhu JJ. Phospholipase C Beta 1: a Candidate Signature Gene for Proneural Subtype High-Grade Glioma. Mol Neurobiol 2016;53:6511-25.
56. Wang Y, Kong X, Guo Y, Wang R, Ma W. Continuous dose-intense temozolomide and cisplatin in recurrent glioblastoma patients. Medicine (Baltimore) 2017;96:e6261.
57. Enríquez Pérez J, Fritzell S, Kopecky J, Visse E, Darabi A, Siesjö P. The effect of locally delivered cisplatin is dependent on an intact immune function in an experimental glioma model. Sci Rep 2019;9:5632.
58. Ferrari B, Roda E, Priori EC, et al. A New Platinum-Based Prodrug Candidate for Chemotherapy and Its Synergistic Effect With Hadrontherapy: Novel Strategy to Treat Glioblastoma. Front Neurosci 2021;15:589906.
59. Holdhoff M, Kreuzer KA, Appelt C, et al. Imatinib mesylate radiosensitizes human glioblastoma cells through inhibition of platelet-derived growth factor receptor. Blood Cells Mol Dis 2005;34:181-5.
60. Das S, Roy A, Barui AK , et al. Anti-angiogenic vanadium pentoxide nanoparticles for the treatment of melanoma and their in vivo toxicity study. Nanoscale 2020;12:7604-21.
61. Kaley T, Touat M, Subbiah V, et al. BRAF Inhibition in *BRAF*^{V600}-Mutant Gliomas: Results From the VE-BASKET Study. J Clin Oncol 2018;36:3477-84.
62. Nicolaides T, Nazemi KJ, Crawford J, et al. Phase I study of vemurafenib in children with recurrent or progressive BRAF^{V600E} mutant brain tumors: Pacific Pediatric Neuro-Oncology Consortium study (PNOC-002). Oncotarget 2020;11:1942-52.
63. Del Bufalo F, Ceglie G, Cacchione A, et al. *BRAF* V600E Inhibitor (Vemurafenib) for *BRAF* V600E Mutated Low Grade Gliomas. Front Oncol 2018;8:526.

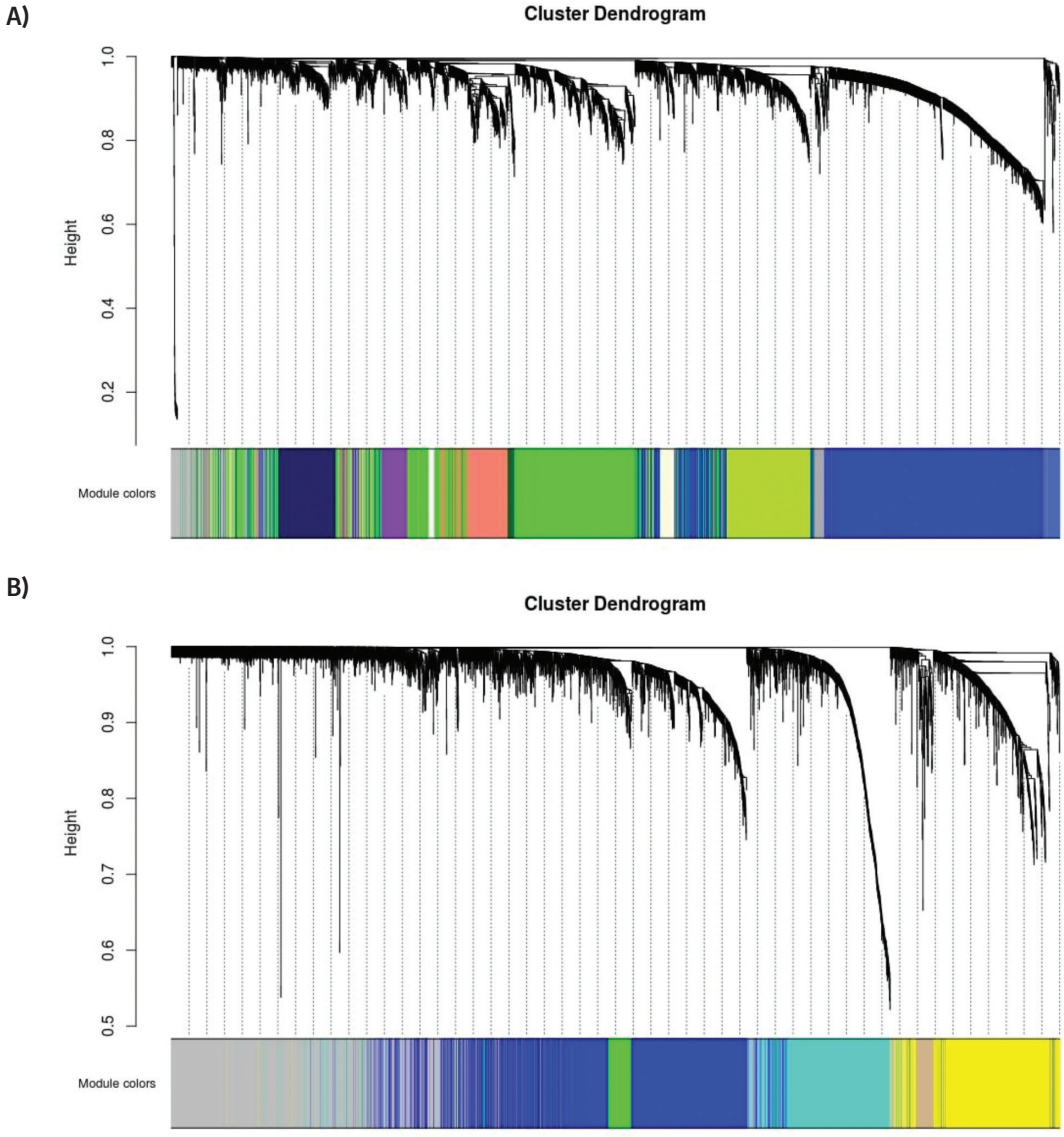


Supplementary Figure 1. Sample clustering of TCGA LGG IDHmt samples by average methodology **A)** IDHmt samples, **B)** IDHwt samples

TCGA: The Cancer Genome Atlas, LGG: Lower-grade glioma, IDHmt: Isocitrate dehydrogenase mutated, IDHwt: Isocitrate dehydrogenase wild-type, e: 10^, branches reflect the patient barcodes



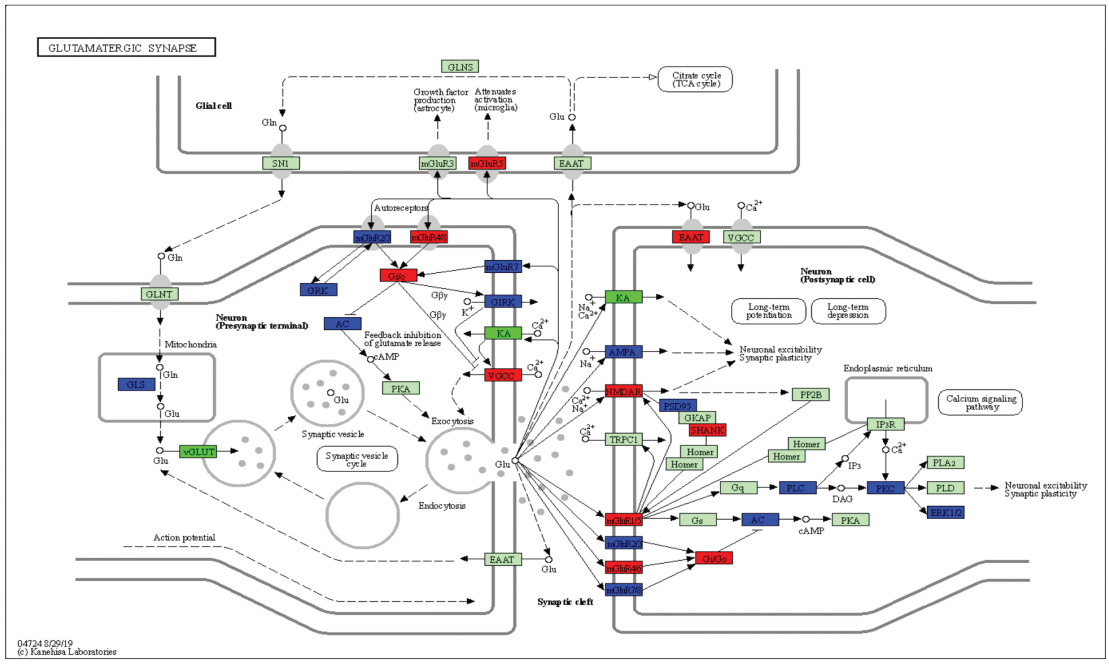
Supplementary Figure 2. Network topology analysis for soft-thresholding powers. **A)** IDHmt samples, **B)** IDHwt samples
IDHmt: Isocitrate dehydrogenase mutated, IDHwt: Isocitrate dehydrogenase wild-type



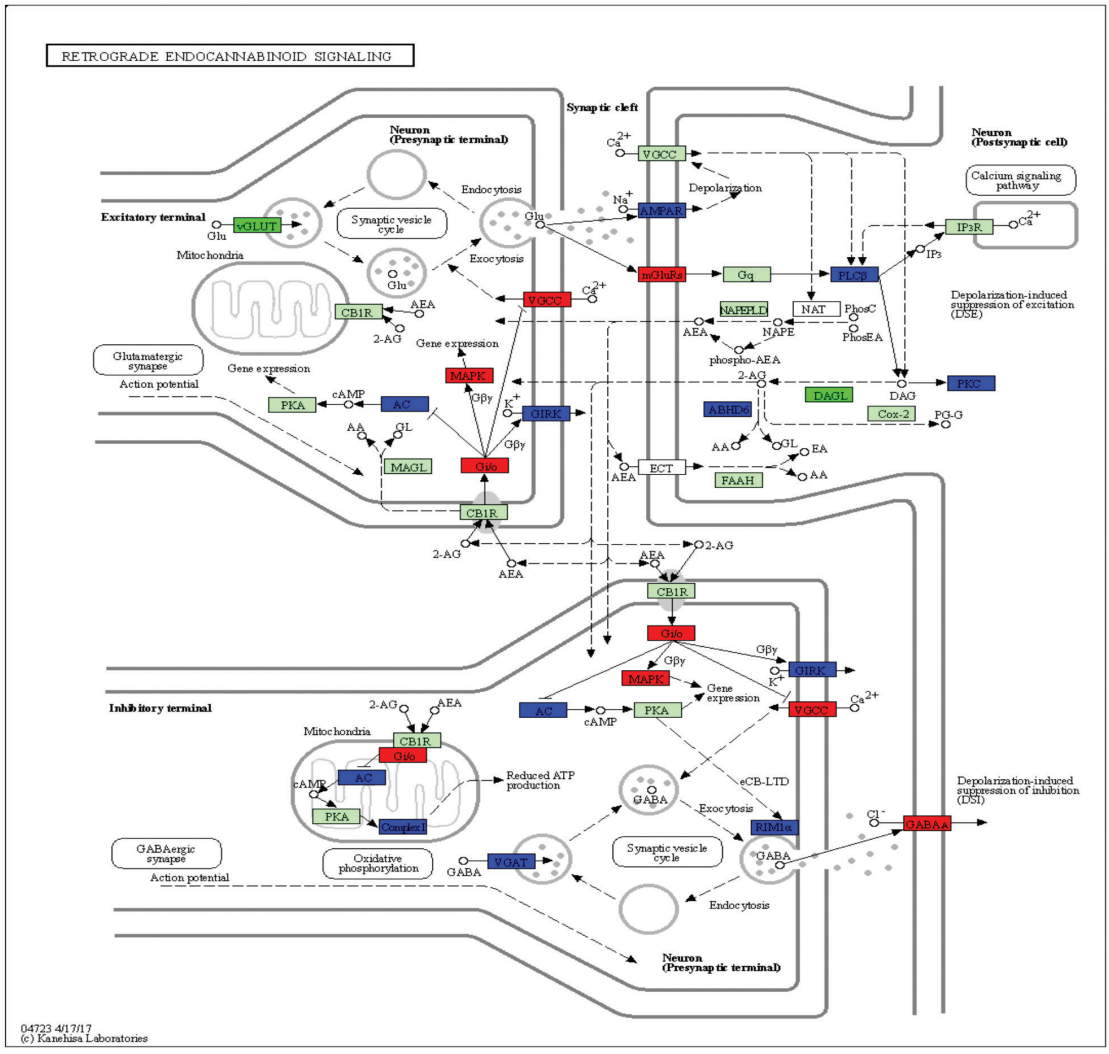
Supplementary Figure 3. Hierarchical clustering of genes with module colors **A)** IDHmt samples, **B)** IDHwt samples

IDHmt: Isocitrate dehydrogenase mutated, IDHwt: Isocitrate dehydrogenase wild-type

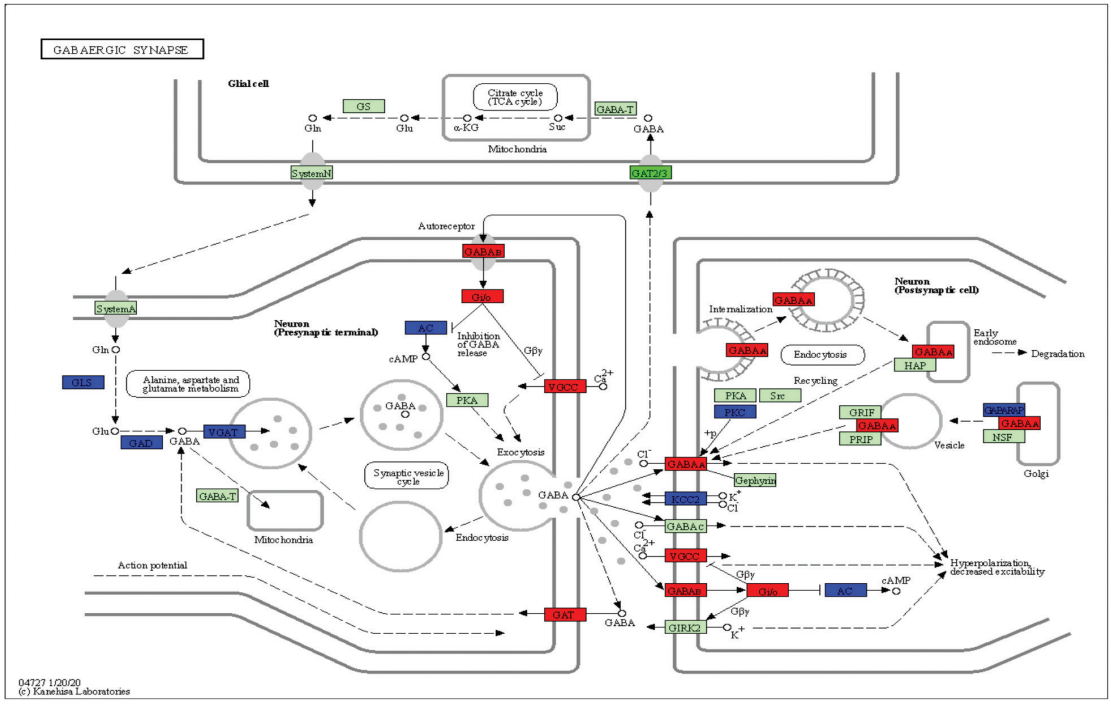
A)


GLUTAMATERGIC SYNAPSE
GLNS
Citrate cycle (TCA cycle)
Glial cell
Growth factor production (astrocyte)
Attenuates activation (microglia)
Gln
Glu
SN1
mGluR3
mGluR5
EAAT
Autoreceptors
mGluR2
mGluR8
Gln
GLNT
Gi/o
GRK
Gβγ
GIRK
K+
AC
Feedback inhibition of glutamate release
cAMP
KA
Ca2+
VGCC
Neuron (Presynaptic terminal)
Mitochondria
GLS
Gln
Glu
vGLUT
Glu
Synaptic vesicle
Synaptic vesicle cycle
Exocytosis
PKA
Endocytosis
Action potential
EAAT
Glu
Synaptic cleft
Glu
Ca2+
EAAT
VGCC
Neuron (Postsynaptic cell)
KA
Na+
Ca2+
Long-term potentiation
Long-term depression
AMPA
Na+
Neuronal excitability
Synaptic plasticity
NMDAR
Na+
Ca2+
PSD95
GKAP
CHANK
TRPC1
Ca2+
Homer
Endoplasmic reticulum
PP2B
IP3R
Calcium signaling pathway
IP3
DAG
Gq
PLC
PKC
PLA2
PLD
ERK1/2
Neuronal excitability
Synaptic plasticity
Gs
AC
cAMP
PKA
04724 8/29/12
(c) Kanehisa Laboratories

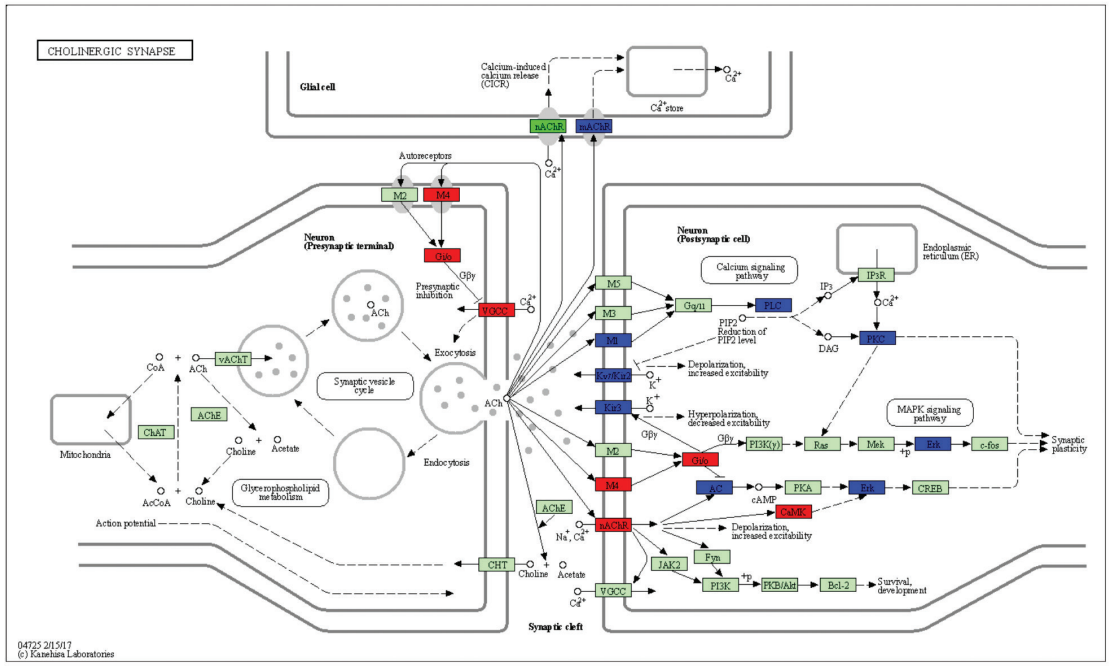
B)


RETROGRADE ENDOCANNABINOID SIGNALING
Synaptic cleft
Neuron (Presynaptic terminal)
Neuron (Postsynaptic cell)
Excitatory terminal
Glu
vGLUT
Synaptic vesicle cycle
Endocytosis
Exocytosis
Mitochondria
Glu
CB1R
AEA
2-AG
Gene expression
Glutamatergic synapse
Action potential
MAPK
PKA
cAMP
AC
Gβγ
K+
GIRK
AA
GL
MAGL
Gi/o
VGCC
Ca2+
Depolarization
AMPAR
Na+
mGluRs
Gq
PLCβ
IP3R
IP3
Calcium signaling pathway
Depolarization-induced suppression of excitation (DSE)
NAPEPLD
NAT
PhosC
PhosEA
NAPE
phospho-AEA
DAGL
DAG
PKC
Cox-2
PG-G
ABHD6
ECT
FAAH
EA
Inhibitory terminal
Mitochondria
Complex I
Reduced ATP production
Oxidative phosphorylation
GABAergic synapse
Action potential
VGAT
GABA
Synaptic vesicle cycle
Endocytosis
eCB-LTD
Exocytosis
RIMs
GABAA
Cl-
Depolarization-induced suppression of inhibition (DSI)
04723 4/17/17
(c) Kanehisa Laboratories

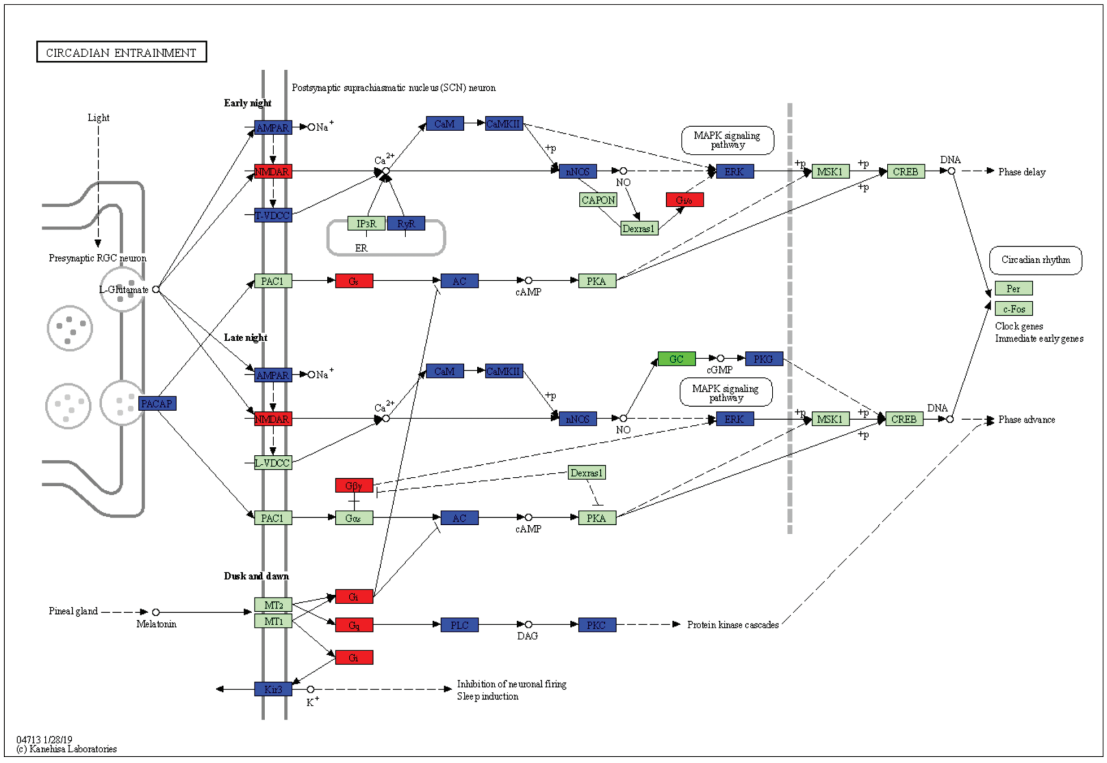
C)


GABAERGIC SYNAPSE
Glial cell
Citrate cycle (TCA cycle)
GS
GABA-T
Gln
Glu
α-KG
Suc
GABA
Mitochondria
SystemN
GAT2/3
Autoreceptor
GABABr
Gi/o
SystemA
Neuron (Presynaptic terminal)
AC
Inhibition of GABA release
cAMP
Gβγ
Ca2+
VGCC
GLS
Alanine, aspartate and glutamate metabolism
Gln
GAD
GABA
VGAT
PKA
Exocytosis
Synaptic vesicle cycle
Endocytosis
Mitochondria
Action potential
GAT
Neuron (Postsynaptic cell)
Internalization
GABAAr
Endocytosis
Recycling
Early endosome
Degradation
HAP
PKA
Src
PKC
GRIF
PRIP
Vesicle
GDP/GTP
NSF
Golgi
Cl-
Gephyrin
GABAc
GIRK2
K+
Hyperpolarization, decreased excitability

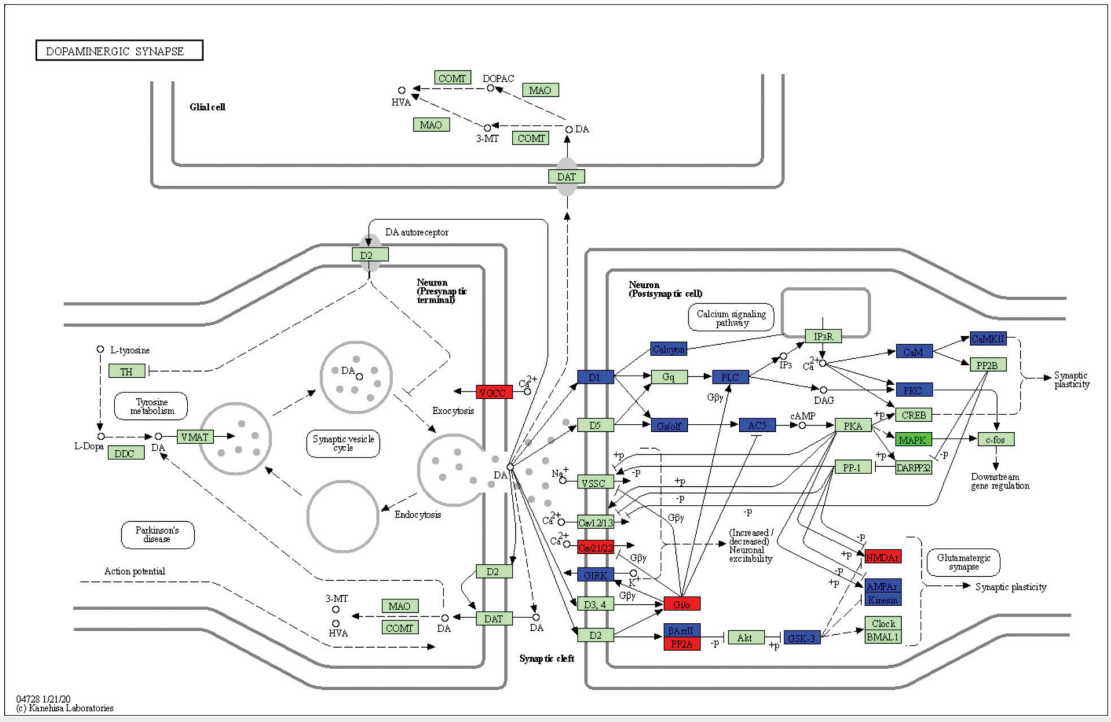
D)


CHOLINERGIC SYNAPSE
Glial cell
Calcium-induced calcium release (CICR)
Ca2+ store
nAChR
Autoreceptors
M2
M4
Neuron (Presynaptic terminal)
Gi/o
Gβγ
Presynaptic inhibition
VGCC
ACh
Exocytosis
Synaptic vesicle cycle
vAChT
CoA
AcCoA
ChAT
Mitochondria
AChE
Choline
Acetate
Glycerophospholipid metabolism
Endocytosis
Action potential
CHT
Neuron (Postsynaptic cell)
Calcium signaling pathway
M5
M3
M1
Kir3/GIRK2
Kv1
Gq/11
PLC
PIP2
Reduction of PIP2 level
Depolarization, increased excitability
Hyperpolarization, decreased excitability
PI3K(γ)
Ras
Mek
Erk
c-fos
MAPK signaling pathway
Synaptic plasticity
AC
cAMP
PKA
CREB
CaMK
Fyn
JAK2
PI3K
PKB/Akt
Bcl-2
Survival, development
Endoplasmic reticulum (ER)
IP3R
IP3
DAG
Synaptic cleft

E)



F)



Supplementary Figure 4. Selected common KEGG pathway schemes of the IDHwt pTERT- blue module and IDHmt pTERT+ greenyellow module. **A)** Glutamatergic synapse, **B)** Retrograde endocannabinoid signaling, **C)** GABAergic synapse, **D)** Cholinergic synapses, **E)** Circadian entrainment, **F)** Dopaminergic synapse

IDHmt: Isocitrate dehydrogenase mutated, IDHwt: Isocitrate dehydrogenase wild-type, pTERT: Telomerase Reverse Transcriptase promoter. Pathway sub-components colored in blue are enriched in the blue module but not in the greenyellow module; pathway sub-components colored in green are enriched in the greenyellow module but not in blue module; pathway sub-components colored in red are enriched in both modules